Ingenious Digital Speed Controller for Switched Reluctance Motor Drives

S. Paramasivam, R. Arumugam, and N. Muthukumaran

Abstract—**In this paper, an ingenious digital speed control scheme for a Switched Reluctance Motor (SRM) drive is presented. It is based on discrete P, PI and PID control algorithms. The scheme is implemented by using a ADμC812 flash microcontroller. The real time experimental results given in this paper show that the speed control method proposed could provide accurate speed control over a wide range of speeds and can also perform accurately at different operating conditions (steady state/transient operation under soft chopping mode). The closed-loop SRM speed control system is seen to achieve ±1 RPM speed accuracy. Complete descriptions of the experimental system along with software operating instructions are presented.**

Index Terms—**Switched reluctance motor (SRM), speed control, discrete P, PI, and PID controllers and microcontrollers.**

I. INTRODUCTION

THE INCREASING popularity of the switched reluctance motor drive (SRM) is mainly due to the fact that its speed torque characteristics can be tailored to meet any specific operating requirement. SRM drives have been used for many years in applications, where simplicity of construction was primary importance. The SRM has salient poles on both the rotor and the stator, but only the stator poles carry windings. The rotor tries to get to a position of minimum reluctance by aligning itself with the stator magnetic field when the stator winding are excited. Thus, exciting the stator phase windings of the motor in a particular sequence and consequently, controlling the magnetic field, the movement of the rotor can be controlled. The availability of low cost power semiconductor switches, dedicated digital controllers and excellent speed torque characteristics of the SRM have paved the way for the applications of these machines to more demanding industrial applications. The advantages like less weight, higher efficiency also favors these machines are more suitable to electric vehicles and aircrafts [1], [2]. The controller for this kind of motors is normally provided with complex analog circuits, which are bulky, costly and not reliable. Hence, the implementation of a low cost digital speed control of SRM using ADμC812 kit with a simplified design, reduced circuit areas and parts count compared to the conventional controllers is desired. Many papers have been reported on the performance simulation of SRM with experimental validation for different control strategies such as feed back linearization control, variable structure control, fuzzy logic control and four-quadrant operation of SRM [3]-[6]. None of these papers have focused exclusively on reduction of speed error and settling time under various operating conditions. This paper is organized as follows. Section II reviews the SRM description. Section III describes the digital controller implementation. Section IV discusses the experimental setup. Section V explains the results obtained during experimentation. Section VI presents the conclusion.

Manuscript received May 17, 2004; revised October 10, 2004.

The authors are with the Department of Electrical and Electronics Engineering, Anna University, Chennai-600025, India (email: paramsathya@yahoo.com).

Publisher Item Identifier S 1682-0053(05)0283

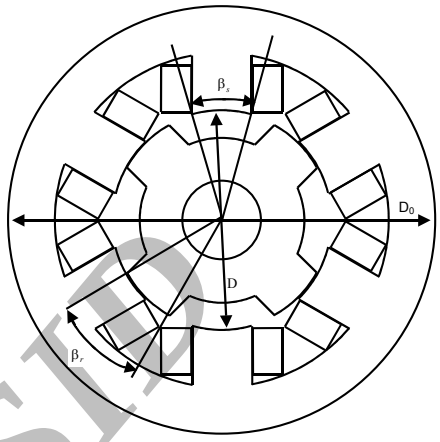

Fig. 1. A 6/4 Pole prototype SRM.

II. SRM DESCRIPTION

Fig. 1 illustrates the proto type SRM under study. The motor parameters are given in Appendix. It is a six-stator-pole to four-rotor-pole (6:4) motor. This motor can be run only from dc supply. The diametrically opposite stator poles are excited simultaneously. The switching sequence of the stator phase is determined by the rotor position sensors or using any suitable indirect rotor position sensing techniques.

The inductance of the excited stator winding thus varies with the varying reluctance of the air gap, reaching a maximum at the aligned position and a minimum at the unaligned position. The inductance at any instant is dependent on both the rotor position and the phase current. The Inductance (L) variation over one rotor pole pitch with constant current magnitude is shown in Fig. 2. The most general expression for the torque produced by one phase at any rotor position is given by [1]-[3]

$$T = \left.\frac{\partial W_c}{\partial \theta}\right|_{i=cont.} \tag{1}$$

where W_c is the co energy defined as

$$W_c = \int_0^i \psi di \tag{2}$$

i and θ are the phase current and the rotor position, respectively.

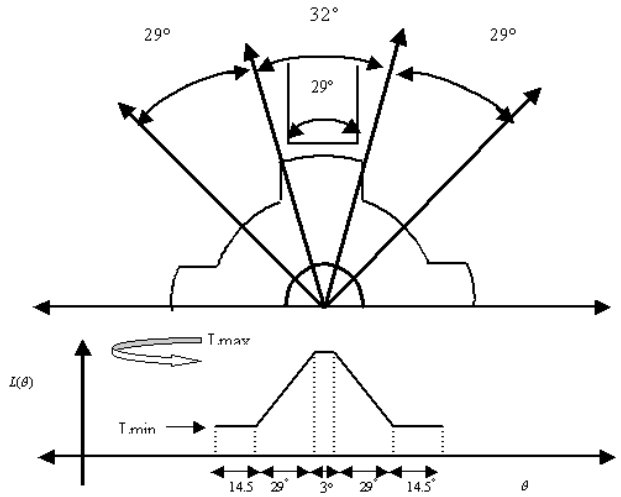

Fig. 2. Inductance profile for one rotor pole pitch.

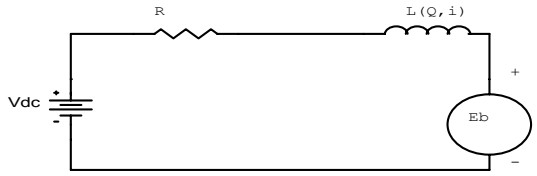

Fig. 3. Per phase electrical equivalent circuit of SRM.

The per phase equivalent circuit of the SRM can be drawn as shown in Fig. 3.

$$V(t) = Ri(t) + L(\theta, i)\frac{di}{dt} + i\varpi\frac{dL(\theta, i)}{d\theta} \quad (3)$$

where V and R are the voltage applied to the phase and the phase resistance, respectively. In this equation, the left side terms are the resistive voltage drop, the static and motional voltages, respectively.

Equation (3) is valid only when the mutual inductances are neglected. From the above equation, it is understood that the motional voltage of each phase is proportional to the speed and rate of change of inductance with respect to rotor position. To get the motoring operation, it is required to energize the stator phase windings at increasing inductance rotor position [1], [2]. The exact choice of the turn-on and turn-off angles, determine the ultimate performance of the SRM. In order to implement the control algorithm effectively, a digital controller has to be implemented. The basic block diagram of closed loop speed control system and SRM drive is shown in Fig. 4.

III. Digital Controller Implementation

In general, digital controllers can be implemented as digital filters in the following form [17], where k is the current sample in time, for a given sample period T

$$y(k) = \sum_{i=0}^{n} a_i x(k-i) - \sum_{i=1}^{n} b_i y(k-i) \quad (4)$$

When $n = 2$ in (4), a second order filter is obtained which can be used to implement second order controllers. This representation for a second order discrete time controller in the sampled time domain is shown below

$$y(k) = a_0 x(k) + a_1 x(k-1) + a_2 x(k-2) - b_1 y(k-1) - b_2 x(k-2) \quad (5)$$

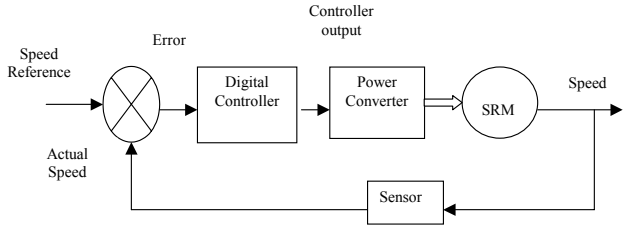

Fig. 4. Closed loop speed control system.

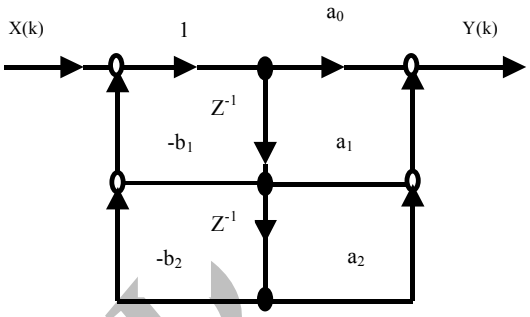

Fig. 5. Signal flow graph of the second order discrete controller.

In this form $y(k)$ is the output, $x(k)$ is the input, a_i and b_i are gains of the controller. These gains must be selected to produce the desired controller output for a given SRM to be controlled. The structure of the second order digital controller is illustrated in Fig. 5. In this figure, the Z^{-1} blocks represent delays of one sample period. The Z^{-1} transform of (5) gives the following transfer function

$$D(z) = \frac{Y(z)}{X(z)} = \frac{a_0 + a_1 z^{-1} + a_2 z^{-2}}{1 + b_1 z^{-1} + b_2 z^{-2}}. \quad (6)$$

These kinds of second order controller are generally implemented through micro controllers or digital signal processors. In this paper, speed control of SRM utilizes the P, PI and PID algorithms [18]-[20]. The proportional control mode gives rapid closed loop transient response to step changes in the speed reference and fast rejection of speed disturbances. The integral control mode assures that the final SRM speed will match the speed reference. The derivative control mode reduces transient overshoot and oscillation in the speed when the reference is changed from one value to another. The P, PI and PID algorithm can be expressed in the discrete-time domain as

(i). Discrete proportional (P) controller

$$u(k) = K_P e(k). \quad (7)$$

(ii). Discrete proportional and integral controller (PI)

$$u(k) = K_P e(k) + \frac{T}{K_I} S(k). \quad (8)$$

(iii). Proportional, integral controller and derivative controller (PID)

$$u(k) = K_P e(k) + \frac{T}{K_I} S(k) + K_D \frac{e(k) - e(k-1)}{T}. \quad (9)$$

where

$u(k)$ is the control signal
$e(k)$ is the error signal
T is the sample period
K_P is the proportional mode control gain
K_I is the integral mode control gain
K_D is the derivative mode control gain.

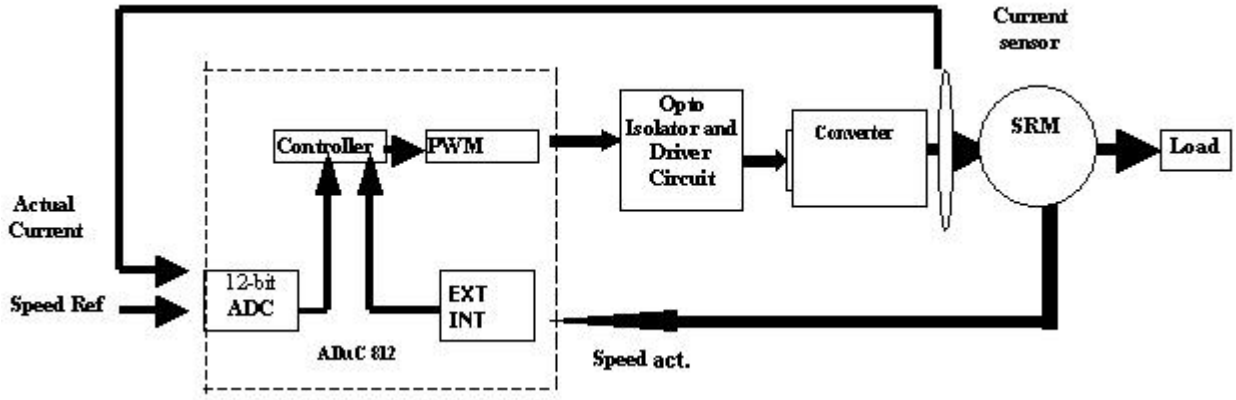

Fig. 6. Experimental system block diagram of the speed controller for the SRM.

TABLE I
SIGNAL FROM SENSORS AND COMMUNICATION LOGICS

Degrees	A	B	C	NORMAL			BOOST			ALD			BRAKE		
				1	2	3	1	2	3	1	2	3	1	2	3
0-7.5	1	1	0	0	0	1	0	0	1	0	1	0	1	0	0
7.5-15	0	1	0	0	0	1	0	1	0	0	1	1	1	0	0
15-22.5	0	1	0	0	0	1	0	1	0	0	1	1	1	0	0
22.5-30	0	1	1	0	1	0	0	1	0	1	1	1	0	0	1
30-37.5	0	1	1	0	1	0	0	1	0	1	1	1	0	0	1
37.5-45	0	0	1	0	1	0	1	0	0	1	0	1	0	0	1
45-52.5	0	0	1	1	1	0	1	0	0	1	0	1	0	0	0
52.5-60	1	0	1	1	0	0	1	0	0	1	0	0	0	1	0
60-67.5	1	0	1	1	0	0	1	0	0	1	0	0	0	1	0
67.5-75	1	0	0	1	0	0	0	0	1	0	0	0	0	1	0
75-82.5	1	0	0	0	0	0	0	0	1	0	0	0	0	1	0
82.5-90	1	1	0	0	0	1	0	0	1	0	1	0	1	0	0

To eliminate the need to calculate the full summation in each time step the summation is expressed as a running sum

$$S(k) = S(k-1) + \frac{T}{2}(e(k) + e(k-1)) \,. \tag{10}$$

The z-transform of discrete PID controller gives the transfer function

$$D(z) = K_P + \frac{K_I T}{2}\left(\frac{z+1}{z-1}\right) + \frac{K_D}{T}\left(\frac{z-1}{z}\right) = \frac{a_0 + a_1 z^{-1} + a_2 z^{-2}}{(1 - b_1 z^{-1} + b_2 z^{-2})} \tag{11}$$

where the following parameters are the gains of the digital controller

$$a_0 = K_P + \frac{K_I T}{2} + \frac{K_D}{T},\ a_1 = -K_P + \frac{K_I T}{2} - \frac{2K_D}{T}$$

$$a_2 = \frac{K_D}{T},\ b_1 = -1,\ b_2 = 0$$

The algorithm developed in the discrete time domain has been implemented through a ADμC812 flash microcontroller. The complete assembly program for PID control algorithm is given in Appendix-B.

IV. EXPERIMENTAL SETUP

A. Hardware

Fig. 6. Shows the block diagram of the system setup of the speed controller for switched reluctance motor. The function of each block is described in this subsection.

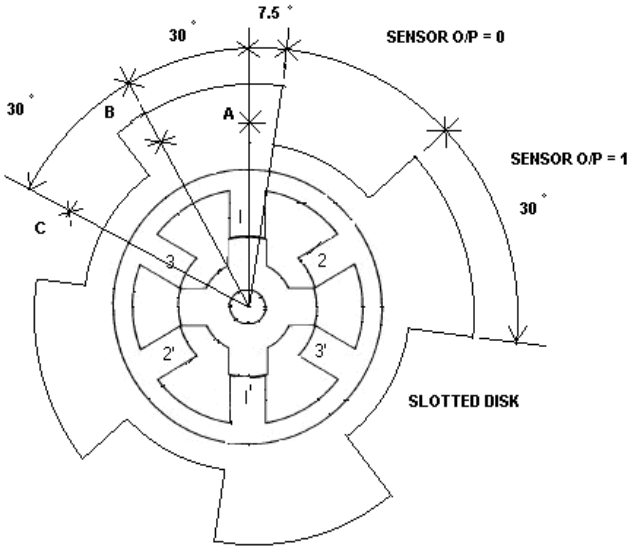

Fig. 7. Rotor position sensor.

1) Rotor Position Sensor

The SRM requires position sensors for its operation. The position sensors consist of a segmented disk (4 segments) and three sensors each consisting of one MLED 930 (IRLED) and MRD5009 mounted 30 from each other. The segmented disc is mounted on the motor shaft. The complete arrangement of rotor position sensor arrangement is shown in Fig. 7. The signals obtained form the sensors and commutation logic for different modes such as NORMAL, BOOST, ALD and BRAKING are presented in Table I.

2) Power Converter

The power converter with two independent power switches and fast recovery diodes per motor phase is the most used topology. Such a power converter for a 3-phase SRM's is shown in Fig. 8. This converter enables control of the individual phases fully independent on each other and thus permits the full freedom of control. It is proved that this particular converter topology is fault tolerant and suitable for high voltage applications [21]. In this research, IRFP360LC, a 400 V and 23 A power MOSFET and MUR3060, 600 V, 30 A "ultra fast diodes" are chosen as the main switching device and freewheeling diode for the converter. All the devices are mounted on the heat sink and the interconnections made on a PCB.

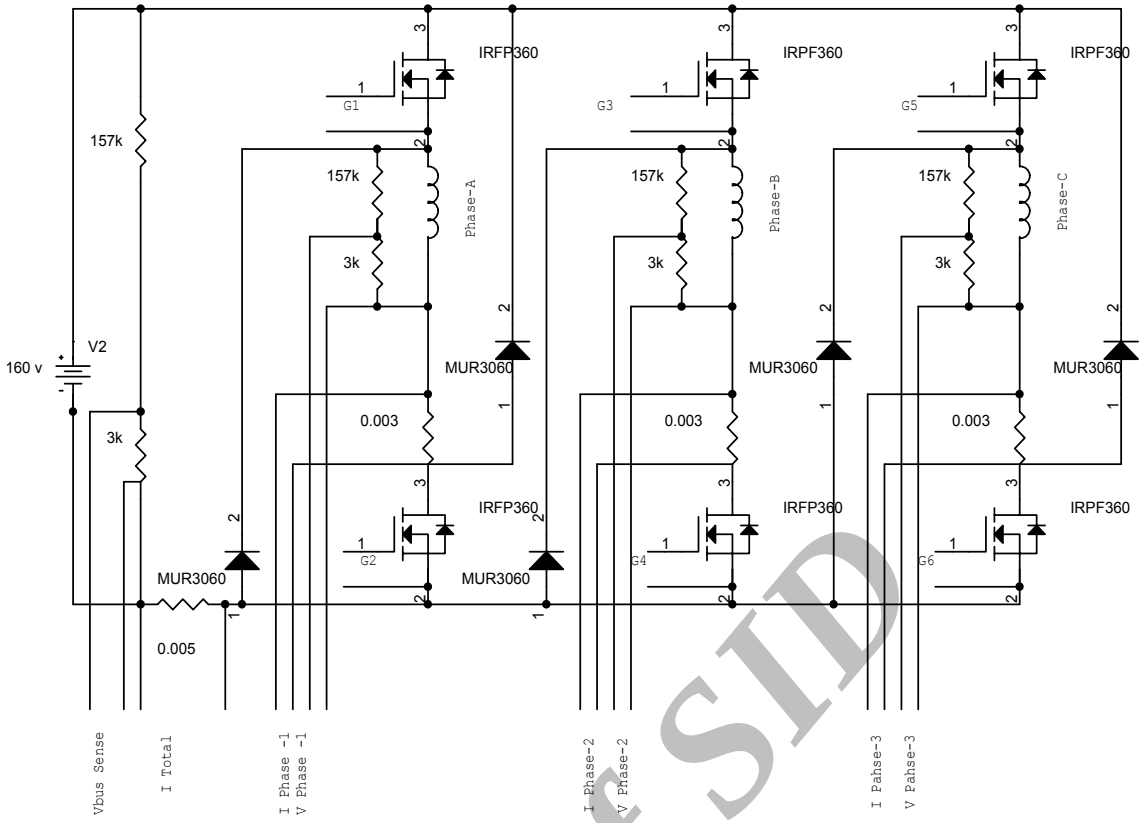

Fig. 8. Classic bridge SRM converter along with sensor arrangement.

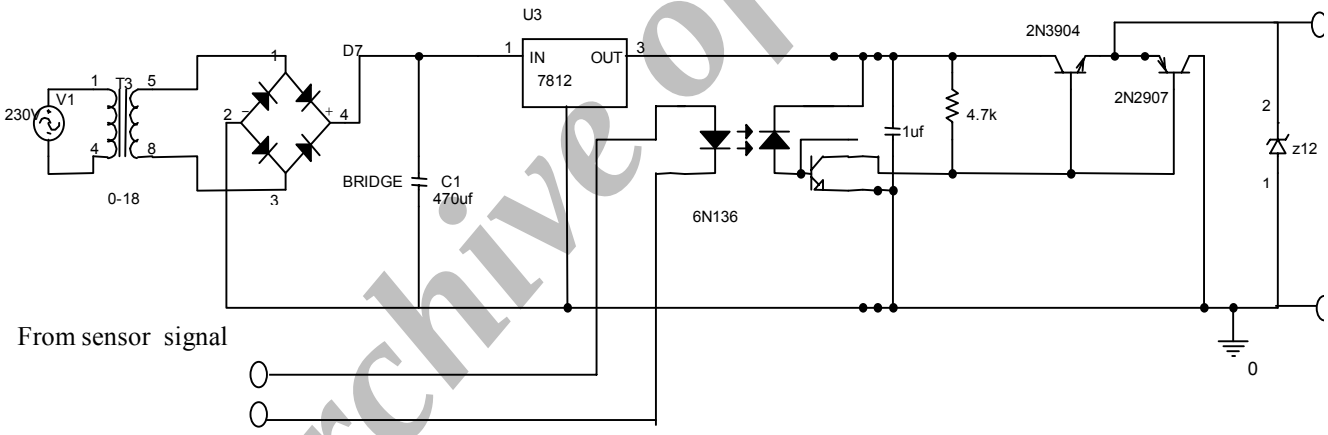

Fig. 9. Classic bridge SRM converter along with sensor arrangement.

3) *Gate Driver and Optoisolator*

The gate drivers get the signal pulses from the microcontroller board and amplify them to the level required for switching the power MOSFETs. The discrete totem pole gate drive circuit is used to drive the MOSFETs. To turn the MOSFET ON, the input to the driver is OFF, thus turning the NPN Transistor ON, which provides a positive gate voltage to the MOSFET and to turn-OFF of the device, the gate is shorted to the source through R_g and PNP transistor. The drive circuit requires isolated DC power supplies. The output of the gate driver is connected across the gate and source of the power MOSFET. The source terminal of the upper MOSFET is floating and thus it can either be at 0 V or at 160 V. As this is connected to the gate driver ground, this floating ground would generate lot of common mode noise. This would interfere with the normal operation of the circuit and it might malfunction. To overcome this situation, the ground of each gate driver

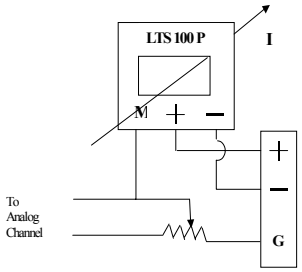

Fig. 10. Current sensing circuit.

output is isolated from the grounds of the other gate driver and also from the input stage ground. The input-output isolation is achieved by using an opto-coupler 6N136 to transfer the control signal from the input buffer stage to the gate driver stage. Further, an isolated DC/DC converter ensures that the grounds of each gate driver circuit are isolated from the other. The complete gate driver and opto-isolator circuit for one switch of the converter is given in Fig. 9.

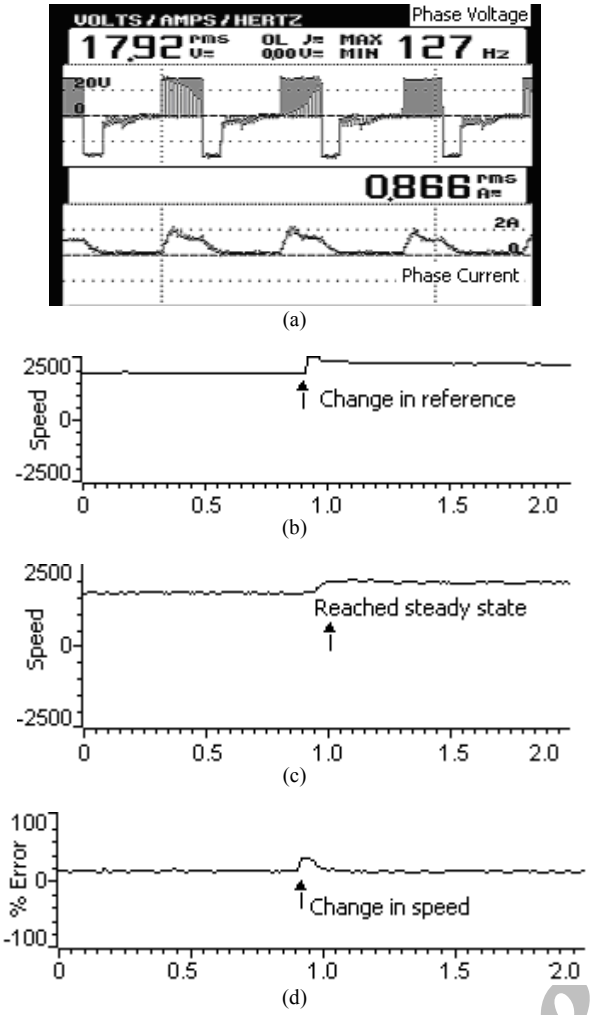

Fig. 11. Measured (a) Phase voltage in volts, phase current in amps, (b) Reference speed in RPM, (c) actual speed in RPM, and (d) % speed error during change in reference speed at t=0.90th sec with no load on P control mode.

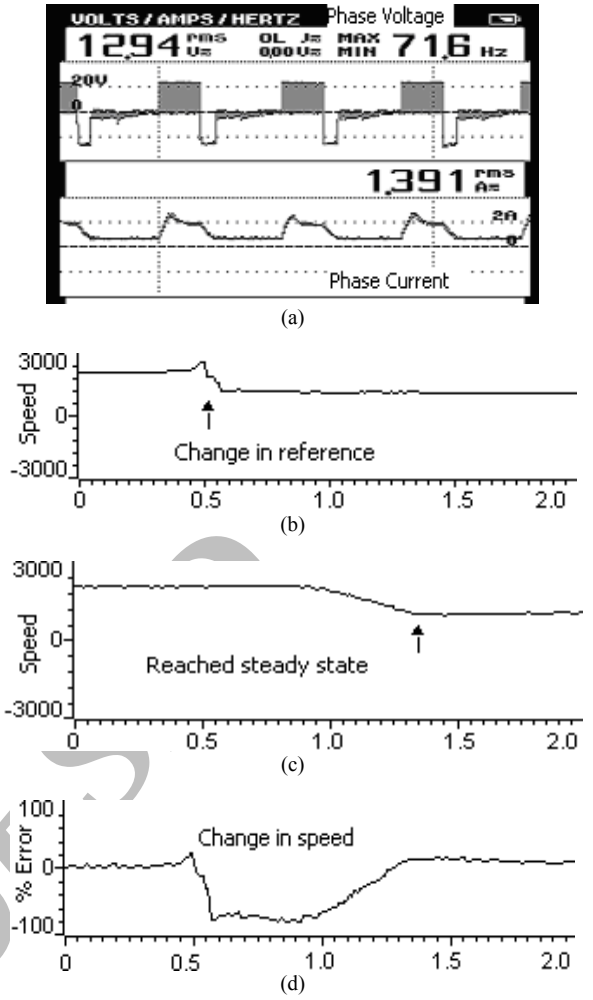

Fig. 12. Measured (a) Phase voltage, phase current, (b) Reference speed, (c) actual speed and (d) % speed error during change in reference speed at t=0.50th sec with no load on PI control mode.

4) Current Sensing Circuit

In order to maintain the current at desired value, the actual phase current is measured through current sensing circuit. In this paper, LTS100P Hall effect current transducer is used and the same circuit is shown in Fig.10.

5) ADμC 812 KIT

The ADμC 812 kit is available from analog devices as development kit. The ADμC 812 kit includes 8051 core, ICL232 for serial communication to PC, cross talk assembler and LABVIEW tool for downloading the HEX files. The microcontroller board itself has three I/O ports to interface with other system hardware. The ADμC 812 board has eight analog channels that are connected through the Port 1 pins. This controller unit support some special functions ADC DMA function, and SPI [22].

B. Software

The implementation of closed loop speed control operation requires the information about the actual speed of the motor. This can be obtained by realizing a frequency to voltage converter circuit or by using the edge-detecting feature of microcontroller. In this paper, an Edge detecting feature is used to detect the negative edge of the rotor position sensor. As and when the negative edge of rotor position sensor is detected, the control is switched to ISR.

The timer starts counting when the negative edge is detected and stops counting when the negative edge is detected form same rotor position sensor. The time interval between two negatives edges is used to calculate the actual speed of the motor. The external interrupt pin INT0 is used to realize the speed measurement algorithm. The reference speed is fed to ADC_channel_0. The reference speed value is from 0-5.0 volts, which corresponds 0-3000 rpm. The values obtained from the ADC and Capture unit is given to the discrete P, PI and PID control algorithm. The output of each discrete controller blocks is taken separately to generate the duty ratio of the PWM signals.

V. Results and Discussion

The speed control systems is built and tested to evaluate the performance of discrete P, PI and PID control algorithm. A prototype MOSFET based classic bride converter is fabricated to energize the 6/4-pole motor. Digital controller is implemented through ADμC812 Flash microcontroller.

Figs. 11-16 shows the experimental results of measured phase voltage, phase current, reference speed, actual speed and % speed error in P, PI and PID control modes during steady state/transient operation under soft chopping operation (X-axis represents time in sec/100). In all the cases the dwell angle is kept constant at 30 degrees. In the P control mode, results have shown that, a steady state

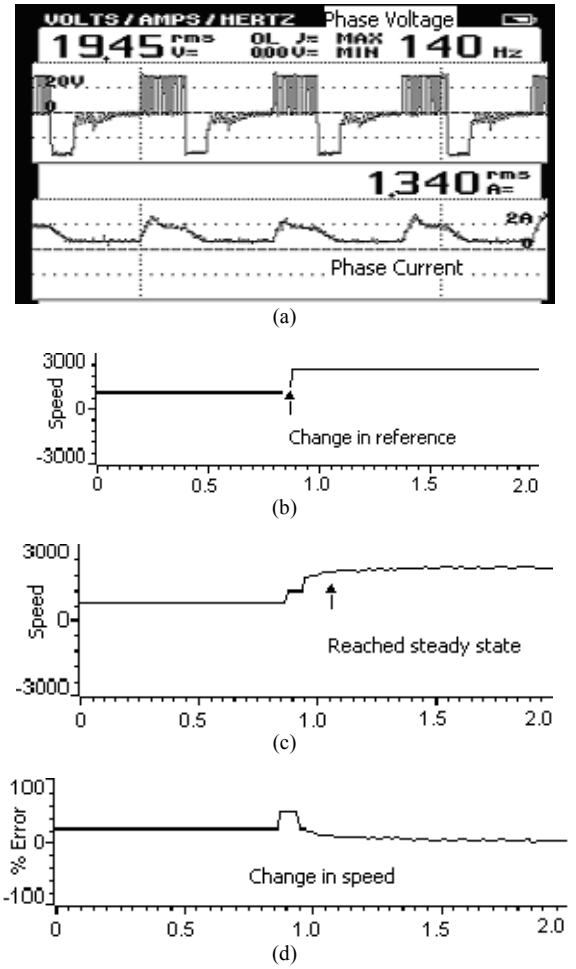

Fig. 13. Measured (a) Phase voltage, phase current, (b) Reference speed, (c) actual speed and (d) % speed error during change in reference speed at t=0.80th sec with no load on PID control mode.

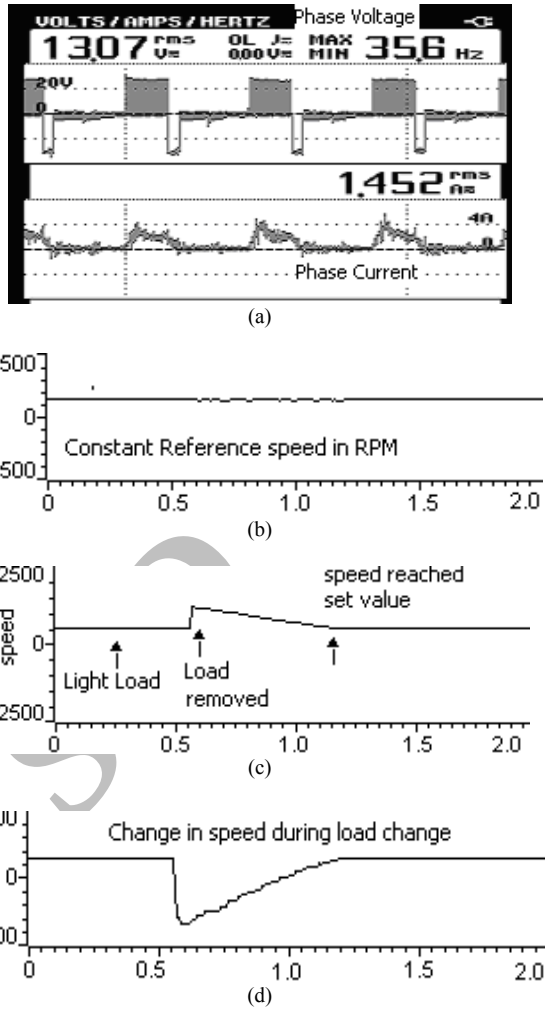

Fig. 14. Measured (a) Phase voltage, phase current, (b) Reference speed, (c) actual speed and (d) % speed error during load change at t=0.56th sec with constant reference speed on P control mode.

error is always present on no load and loaded conditions. In the PI control mode, results have shown that, the steady state error becomes zero after 0.75 seconds on no load and 1.05 seconds loaded conditions. In the PID control mode, results have shown that, the steady state error becomes zero after 0.4 seconds on no load and 0.25 seconds on loaded conditions. It is found form the experimental results, in PI control mode no chattering effect is present and PID control mode little chattering effect is present. From the above discussion, it is concluded that PI controller is more suitable for steady state operation and PID is more suitable for transient state operation.

VI. Conclusion

In this paper, a robust speed controller for a switched Reluctance motor drive using a digital controller has been developed and implemented based on a three-phase classic bridge converter. The controller employs discrete P, PI and PID speed controllers. Experimental results in this paper show that dc bus voltage is used to successfully control a three-phase 6/4 pole switched reluctance motor drive system to obtain robust speed holding capability, even under highly dynamic loads. Under load conditions the speed error was only RPM PI control mode and RPM in PID control mode during steady state. Most significantly, the implementation of this high-performance speed controller needs only and high speed DSP, a few logic IC's, and a single current sensor. There is no requirement for any power or voltage sensors. It can be concluded that discrete PI and PID speed controllers are effective in dealing with the highly varying load conditions of the SRM drive system.

Appendix

Motor Parameters

Power	1.2KW
Voltage	160 V
Current	16 A
Stator outer diameter	162 mm
Stator core length	90 mm
Stator inner diameter	80 mm
Shaft diameter	25 mm
No of poles in the stator	6
No of turns/pole	75
Cross-section of the conductor	1.7 sq-mm
Stator pole arc	29 degree
Stator pole height	20 mm
No of poles in the rotor	4
Rotor pole arc	32 degree
Rotor Pole height	15 mm

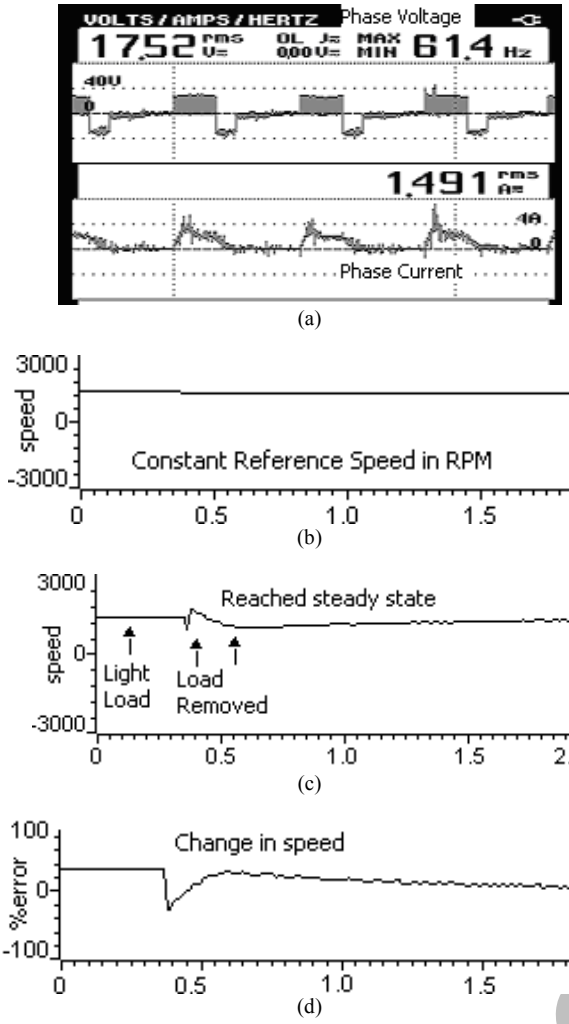

Fig 15. Measured (a) Phase voltage, phase current, (b) Reference speed, (c) actual speed and (d) % speed error during load change at t=0.42nd sec with constant reference speed on PI control mode.

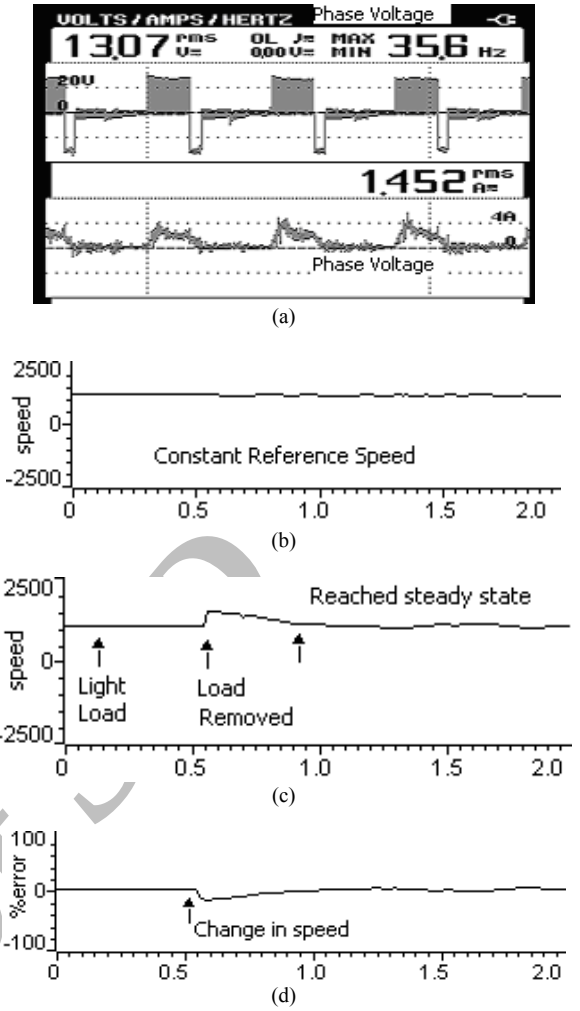

Fig. 16. Measured (a) Phase voltage, phase current, (b) Reference speed, (c) actual speed and (d) % speed error during load change at t= 0.5th sec with constant reference speed on PID control mode.

REFERENCES

[1] T. J. E. Miller, *Brushless Permanent Magnet and Reluctance Motor Drives*, Oxford University Press, 1989.

[2] R. Krishnan, *Switched Reluctance Motor Drives: Modelling, Simulation, Analysis, Design and Applications*, CRC Press, 2001.

[3] J. F. Lindsay, R. Arumugam, and R. Krishnan, "Finite-element analysis of a switched reluctance motor with multi-tooth per stator pole," *Proc. Inst. Elect. Eng., B*, vol. 133, no. 6, pp. 347-353, Nov. 1986.

[4] J. V. Byrne and M. F. McMullion, "Design of a reluctance motor as a 10 kW spindle drive," *in Proc. Motorcon*, pp.10-24, 1982.

[5] B. Powell, *A Low Cost Efficient Motor Driver*, Motornetics Corp., Santa Rose, California, US.

[6] R. Welburn, *Ultra High Torque Motor System for Direct Drive Robotics*, Motornetics Corp., Santa Rose, California, US.

[7] W. F. Ray, P. J. Lawrension, R. M. Davis, J. M. Stephension, N. N. Fulton, and R. J. Bake, "High performance SR brushless drives," *IEEE Trans. on Industrial Applications*, vol. 22, no. 4, pp. 722-730, Jul./Aug. 1986.

[8] C. A. Ferreira, S. R. Jones, W. S. Heglund, and W. D. Jones, "Detailed design of a 30-Kw switched reluctance starter/generator system for a gas turbine engine application," *IEEE Trans. on Industry applications*, vol. 31, no. 3, pp. 553-561, May./Jun. 1995.

[9] C. Hao and X. Guilen, *80C31 Single Chip Computer Control of SRM for Locomotive in Coal Mines*, Chinal University of Mining and Technology, China.

[10] C. Hao, X. Guilin, *80C51 Single Chip Control of SRM for Locomotive in Coal Mines*, China University of Mining and Technology, China.

[11] R. Krishnan and A. S. Bharadwaj, *A Comparative Study of Various Motor Drive Systems for Aircraft Applications*, Motion Control Systems Research Group, Bradley Department of Electrical Engineering, Blacksburg, A 24061-0111.

[12] A. A. Arkadan and B. W. Kielgas, "Switched reluctance motor drive systems dynamic performance prediction and experimental verification," *IEEE Trans. on Energy Conversion*, vol. 9, no.1, pp. 36-44, Mar. 1994,

[13] S. K. Panda and P.cK. Dash, "Application of non-linear control to switched reluctance motors: a feed back approach," *Proc. IEE EPA*, vol. 143, no. 5, pp. 371-379, Sep. 1996.

[14] G. S, Buju, R. Menis, and M. J. Valla, "Variable structure control of an SRM drive," *IEEE Trans. on Industrial Electronics*, vol. 40, no. 1. pp. 56-63, Feb. 1993.

[15] S. Bologani and M. Zigilotto, "Fuzzy logic control for a switched reluctance motor drive," *IEEE Trans. on Industry Applications*, vol. 32, no. 5, pp. 1063-1068, Sep./Oct, 1996.

[16] S. A. Hossain, *et. al*., "Four-quadrant and zero-speed sensorless control of a switched reluctance motor" *IEEE Trans. on Industry Applications*, vol. 39, no. 5, pp. 1343-1349, Sep./Oct, 2003.

[17] C. L. Phillips and H. T. Nagle, *Digital Control System Analysis and Design*, Prentice-Hall, Inc., NJ: Englewood Cliffs, 1984.

[18] K. Astrom and T. Hagglund, *PID Controllers: Theory, Design and Tuning*, 2nd ed., Instrument Society of America, NC: Research Triangle Park, 1995.

[19] H. -P. Huang, M. -L. Roan, and J. -C. Jeng, "On line adaptive tuning for PID controllers", *IEE Proceedings-Control Theory Applications*, vol. 149, no. 1, pp. 60-67, Jan. 2002.

[20] F. Blaabjerg, P. C. Kjaer, P. O. Rasmussen, and C. Cossar, "Improved digital current control methods in switched reluctance motor drives," *IEEE Trans. on Power Electronics*, vol. 14, no. 3, pp. 563-572, May 1999.

[21] M. Sayeed, "Classification of SRM converter topologies for automotive applications," in *Proc. SAE 2000, World Congress*, pp. 1-9, Detroit, Michigan, March 6-9, 2000.

[22] —, *ADuC812: Micro Converter®, Multi Channel 12-Bit ADC with Embedded Flash*, MCU Data Sheet, Rev. E, 4/03.

S. Paramasivam received the B.E. degree from GCT, Coimbatore, in 1995, and the M.E. degree from P.S.G College of Technology, Coimbatore, in 1999, both in electrical engineering. He has submitted his PhD thesis in Anna University, India. His interests include Power Electronics, ac motor drives, DSP and FPGA based motor controls, power-factor correction, and magnetics design.

He is a reviewer for IEEE Transactions on Industrial Applications, Industrial Electronics, Fuzzy Systems, International Journal of Modeling and Simulation, Neuro Computing, Energy Technology and Policy, International Journal of Global Energy Issues.

R. Arumugam received the B.E., M.Sc. (Eng.) degrees in 1969 and 1971 from Madras University, and Ph.D. in 1987 from Concordia University, respectively. At present, he is a Professor and Head of Electrical and Electronics Engineering Department, Anna University, India. He has received many research paper awards. His interests include Computer aided design of Electrical Machines, power electronics, ac motor drives, motor controls, power-factor correction and magnetics design.

N. Muthukumaran the author's biography was not available at the time of journal publication.